Appl Microbiol Biotechnol (2013) 97:6065–6075
DOI 10.1007/s00253-012-4420-6

ENVIRONMENTAL BIOTECHNOLOGY

Changes in biofilm structure during the colonization of chalcopyrite by *Acidithiobacillus thiooxidans*

J. V. García-Meza · J. J. Fernández · R. H. Lara · I. González

Received: 8 June 2012 / Revised: 5 September 2012 / Accepted: 6 September 2012 / Published online: 28 September 2012

Abstract Biofilms of *Acidithiobacillus thiooxidans* were grown on the surface of massive chalcopyrite electrodes (MCE) where different secondary sulfur phases were previously formed by potentiostatic oxidation of MCE at $0.780 \leq E_{an} \leq 0.965$ V (electrooxidized MCE, eMCE). The formation of mainly S^0 and minor amounts of CuS and S_n^{2-} were detected on eMCEs. The eMCEs were incubated with *A. thiooxidans* cells for 1, 12, 24, 48, and 120 h in order to temporally monitor changes in eMCE's secondary phases, biofilm structure, and extracellular polymeric substance (EPS) composition (lipids, proteins, and polysaccharides) using microscopic, spectroscopic, electrochemical, and biochemical techniques. The results show significant cell attachments with stratified biofilm structure since the first hour of incubation and EPS composition changes, the most important being production after 48–120 h when the highest amount of lipids and proteins were registered. During 120 h, periodic oxidation/formation of S^0/S_n^{2-} was recorded on biooxidized eMCEs, until a stable CuS composition was formed. In contrast, no evidence of CuS formation was observed on the eMCEs of the abiotic control, confirming that CuS formation results from microbial activity. The surface transformation of eMCE induces a structural transformation of the biofilm, evolving directly to a multilayered biofilm with more hydrophobic EPS and proteins after 120 h. Our results suggest that *A. thiooxidans* responded to the spatial and temporal distribution and chemical reactivity of the $S_n^{2-}/S^0/CuS$ phases throughout 120 h. These results suggested a strong correlation between surface speciation, hydrophobic domains in EPS, and biofilm organization during chalcopyrite biooxidation by *A. thiooxidans*.

Keywords *Acidithiobacillus thiooxidans* · Chalcopyrite · Biofilms · Electrooxidation · Interfacial analysis

J. V. García-Meza (✉) · J. J. Fernández
Geomicrobiología, Instituto de Metalurgia, UASLP,
Sierra Leona 550, Lomas 2°,
78210, San Luis Potosi, Mexico
e-mail: jvgm@uaslp.mx

R. H. Lara
Facultad de Ciencias Químicas, UJED,
34120, Durango, Mexico

I. González
Área de Electroquímica, Departamento de Química, UAM,
Iztapalapa,
09340, Mexico City, Mexico

Introduction

Previous work demonstrated that biofilms of *Acidithiobacillus thiooxidans* may attach to massive chalcopyrite electrodes (MCEs) as a function of the surface composition, polysulfides (S_n^{2-}) and elemental sulfur (S^0) being the most prone phases to biooxidation (Lara et al. 2012b). The formation of these phases was achieved by previous electrooxidization of MCE surface at the anodic pulse of $0.780 \leq E_{an} \leq 0.965$ V (electrooxidized MCE, eMCE) under specific growth medium conditions for sulfuroxidizing *A. thiooxidans*. Furthermore, at this potential, no secondary nor tertiary phases of sulfur, with low oxidation capacity (as S_n^{2-}, e.g., $Cu_{1-x}Fe_{1-y}S_2$), were formed. After 24 h, the cells form a flat biofilm partially covered by porous covellite (CuS) and S^0, and the biooxidative activity of *A. thiooxidans*, the synthesis and secretion of extracellular polymeric substance (EPS), and its cell division continue. The porosity of the S^0 layer plays a fundamental role in the irreversible attack of chalcopyrite by bioleaching bacteria (Olivera-Nappa et al. 2010); meanwhile, CuS is oxidized by SOM under acidic conditions (Sasaki et al. 2009; Falco et al. 2003), with S^0 and Cu^{2+} being the dominant products (Lee et al. 2008);

finally, *A. thiooxidans* removes the S^0 produced from CuS. However, for a complete picture of the biooxidative processes, it is necessary to assay longer times of residence and study the interfacial conditions of the mineral/biofilm/EPS system and their emergent properties (biological, chemical, and electrochemical).

Since our previous results suggested that the biofilm structure changes due to the chemical speciation of chalcopyrite, the aim of this work is to describe the dynamics of interfacial changes of eMCEs with active S_n^{2-}/S^0 phases during biooxidation by *A. thiooxidans*. The biochemical composition of EPS was analyzed, and changes in the biofilm structure during bacterium/mineral interaction were followed. A set of combined methods were used: atomic force microscopy (AFM), confocal laser scanning microscopy (CLSM), scanning electron microscopy (SEM), electrochemical techniques, and Raman spectroscopy, as well as biochemical analysis of EPS.

Materials and methods

Mineral and potentiostatic oxidation of MCEs

Chalcopyrite samples were obtained from Charcas, San Luis Potosi, Mexico; the chalcopyrite content of the sample was ~99.6 wt.%, with ~0.2 % of pyrite (FeS_2) and ~0.2 % of quartz (SiO_2), according to a chemical analysis of total digested samples (EAA, Perkin Elmer-1100). The combination of X-ray diffraction patterns and SEM coupled to energy dispersive X-ray spectroscopy confirmed the mineral composition and the presence of impurities as inclusions. Crystal samples of chalcopyrite were selected for the construction of massive chalcopyrite electrodes: mineral coupons of about 1.2 to 1.5 cm^2 were mounted in epoxy resin with a silver epoxy electrical contact on the backside, and the MCE surface (pristine or unoxidized) was polished until a mirror-like surface was obtained.

Electrooxidation of MCE surfaces allows the overproduction of S^0 and S_n^{2-} phases directly. The MCEs were potentiostatically oxidized at 0.86 V/standard hydrogen electrode (SHE) and 3,600 s using an autolab PGSTAT 30 coupled to a PC and a classic Pyrex® glass three-electrode cell; the working electrode was the MCE, the counter electrode was a graphite rod (Alfa *A*esar, 99.9995 % purity), and the reference electrode was a saturated sulfate electrode (0.616 V vs. SHE). The formation of S_n^{2-}/S^0 phases on eMCE surfaces was confirmed by Raman spectroscopy.

A. thiooxidans cultivation

A. thiooxidans (strain ATCC-8085) was cultivated aerobically at 28–30 °C in 50 mL of media ATCC-125 containing 10 g S^0, 3 g KH_2PO_4, 0.4 g $(NH_4)_2SO_4$, 0.5 g $MgSO_4 \cdot 7H_2O$, 0.25 g $CaCl_2 \cdot 2H_2O$, and 0.01 g $FeSO_4 \cdot 7H_2O$ per liter of distilled water. The media was dispensed into 250-mL Erlenmeyer flasks and were sterilized by autoclaving at 121 °C for 15 min. The S^0 was sterilized separately using 2–3 h of UV irradiation with intermittent shaking; sterilization was done by spreading carefully the S^0 over a crystal dish in an active laminar (horizontal) flow cabinet; at every hour, the dispersed S^0 was shaken in order to homogenize the exposure of S^0 grains. If the sterilized S^0 was added to a non-inoculated media, any microorganism grows after 1 week. The final pH of the medium was adjusted to 2 with concentrated H_2SO_4. An inoculum was added to the biotic assays (~10^8 cell/mL).

Biofilms formation

The eMCE was sterilized by exposing to UV irradiation for 24 h; afterward, the eMCE was placed in a flask with 100 mL of ATCC-125 at pH 2 without S^0 source and with ~10^8 cells/mL of *A. thiooxidans*. The culture was incubated aerobically at 28–30 °C and 100 rpm for 1, 12, 24, 48, and 120 h. Biotic assays were done in triplicate. An abiotic control was also carried out in triplicate to compare the chemical and biological oxidation of S^0/S_n^{2-}. After each selected time, the eMCEs were collected, dried with a direct current of nitrogen, and preserved in a desiccator under inert conditions until their analysis.

Surface analysis of eMCEs

The eMCEs' surfaces were analyzed by AFM, CLSM, and Raman spectroscopy to evaluate the evolution of interfacial processes associated with the performed five stages of mineral colonization by *A. thiooxidans*. Before each assay time of contact, observations and analysis of unelectrooxidized MCE and eMCE surfaces before leaching were carried out. After 1, 12, 24, 48, and 120 h of assays, the same analyses were done for biotic (eMCE with *A. thiooxidans*) and abiotic control (eMCE without *A. thiooxidans*).

The AFM analysis was performed with a Nanoscope Multimode IIIa digital instrument in order to visualize biofilms and to obtain roughness (R_a, nm) and root mean square (R_q, nm) data for each eMCE surface using tapping mode in air. Afterward, a triple monochromator Raman Jobin Yvon T64000 spectrometer equipped with an optical microscope (Olympus BH2-UMA) was used for Raman analysis of MCE and eMCEs before leaching and eMCE after biotic and abiotic assays. Further details for AFM and Raman procedure are described in previous works (Lara et al. 2010; González et al. 2012).

After AFM and Raman analysis, the same eMCEs exposed to *A. thiooxidans* (biotic assays) were analyzed by CLSM in

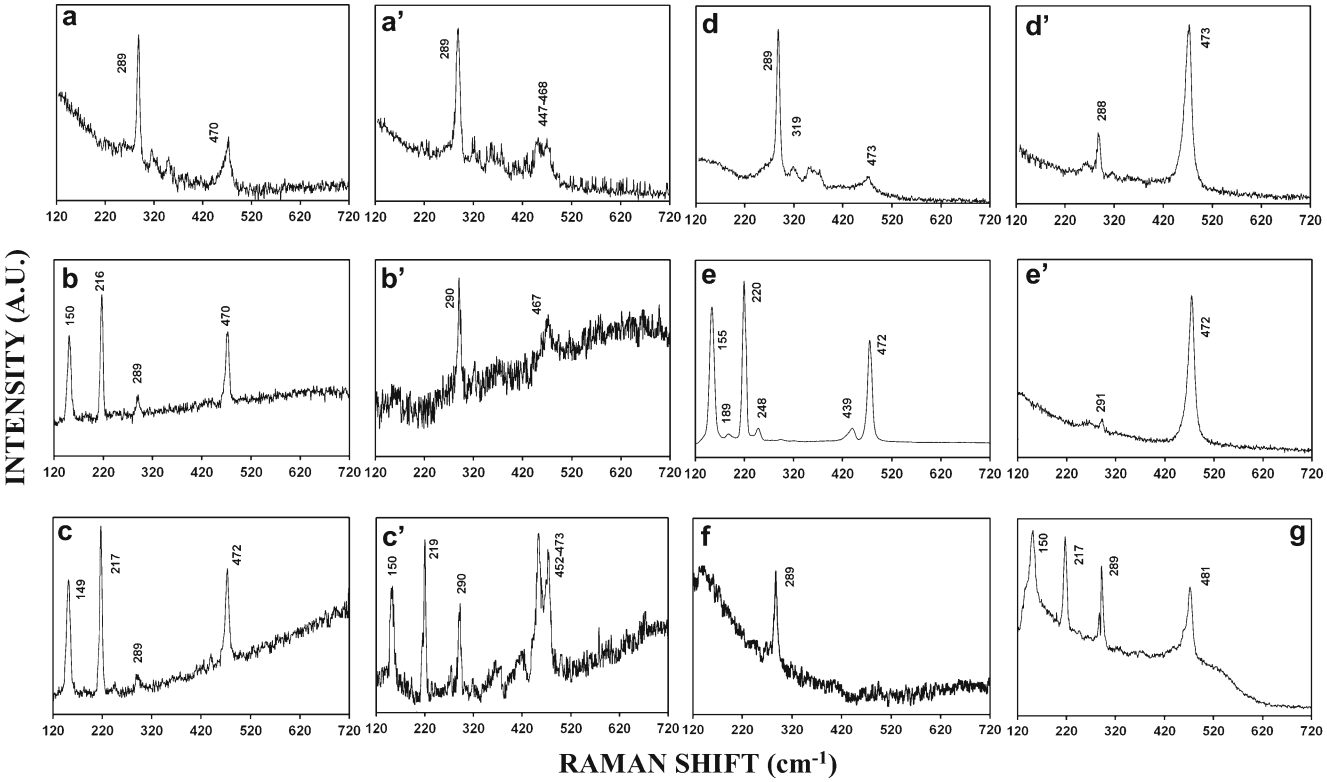

Fig. 1 Raman spectra on previous eMCE; surfaces collected from abiotic control and biotic trials after different immersion times: *a* and a′ 1 h, *b* and *b*) 12 h, *c* and *c*′ 24 h, *d* and *d*′ 48 h, and *e* and *e*′) 120 h. This figure also shows Raman spectra for (*f*) unmodified MCE and (*g*) electrooxidized MCE (without leaching) surfaces for comparison purposes. Collection time of 60 s. λ=521 nm, 20 A

order to detect the epifluorescence signal as indirect strategy to estimate changes in EPS secretion. CLSM observations and analysis were done in biofilms previously fixed and stained with the lectin *Canavalia ensiformis* (Con-A; conjugated tetramethylrhodamine; Molecular Probes, Eugene) for hydrophilic exopolysaccharides (α-mannose and α-glucose) using an excited signal at 488 nm, and the maxima of the emitted signal was detected using a band pass filter for emission at 575 nm. Also, Nile Red (NR; Sigma) fluorochrome was used to stain hydrophobic domains as lipids of EPS using an excited signal at 515–560-nm emission; a band pass filter for emission at 650 nm was used. The difference between the maxima of emitted signals and the corresponding filtering of such signals allowed us to discriminate between exopolysaccharides (stained with Con-A) and hydrophobic domains of EPS (stained with NR). The relative signal intensity of three groups in depth was resolved using the software program of the CLSM (Leica DMI4000B; equipped with argon laser and I3 and N2.1 filters). The data were corrected for background signal. The biofilms were scanned in depth (0.2-μm intervals), allowing for 2D and 3D images to be reconstructed. Finally, the intensity of Con-A and NR fluorescence was used to estimate the relative contribution of extracellular polysaccharides and lipids to EPS; the data were expressed in arbitrary

Table 1 Summary of Raman transitions identification in terms of main sulfur species on MCE and eMCE surfaces

Species	Raman peak position (cm^{-1})	References
Pyrite (monosulfide, S^{-})	344 (*v*2), 380 (*v*1), 433 (*v*3)	Mycroft et al. 1990; Toniazzo et al. 1999; Sasaki et al. 1998; Lara et al. 2012a
Chalcopyrite (monosulfide, S^{-})	292 (*v*1), 320 (*v*2)	Parker et al. 2008; Sasaki et al. 2009
Polysulfides (S_n^{2-})	From 418, 443 to 475, main at 470 (*v*1)	Mycroft et al. 1990; Toniazzo et al. 1999; El Jaroudi et al. 1999, 2000; Turcotte et al. 1993; Parker et al. 2008
Elemental sulfur (S^0)	Main at 155 (*v*3), 220 (*v*2), and 470 (*v*1)	Mycroft et al. 1990; Sasaki et al. 1998; Toniazzo et al. 1999; Xia et al. 2010
Covellite (S^{-})	471 (*v*1), 267 (*v*2), 471 (*v*1)	Parker et al. 2008; Sasaki et al. 2009; Lara et al. 2012b

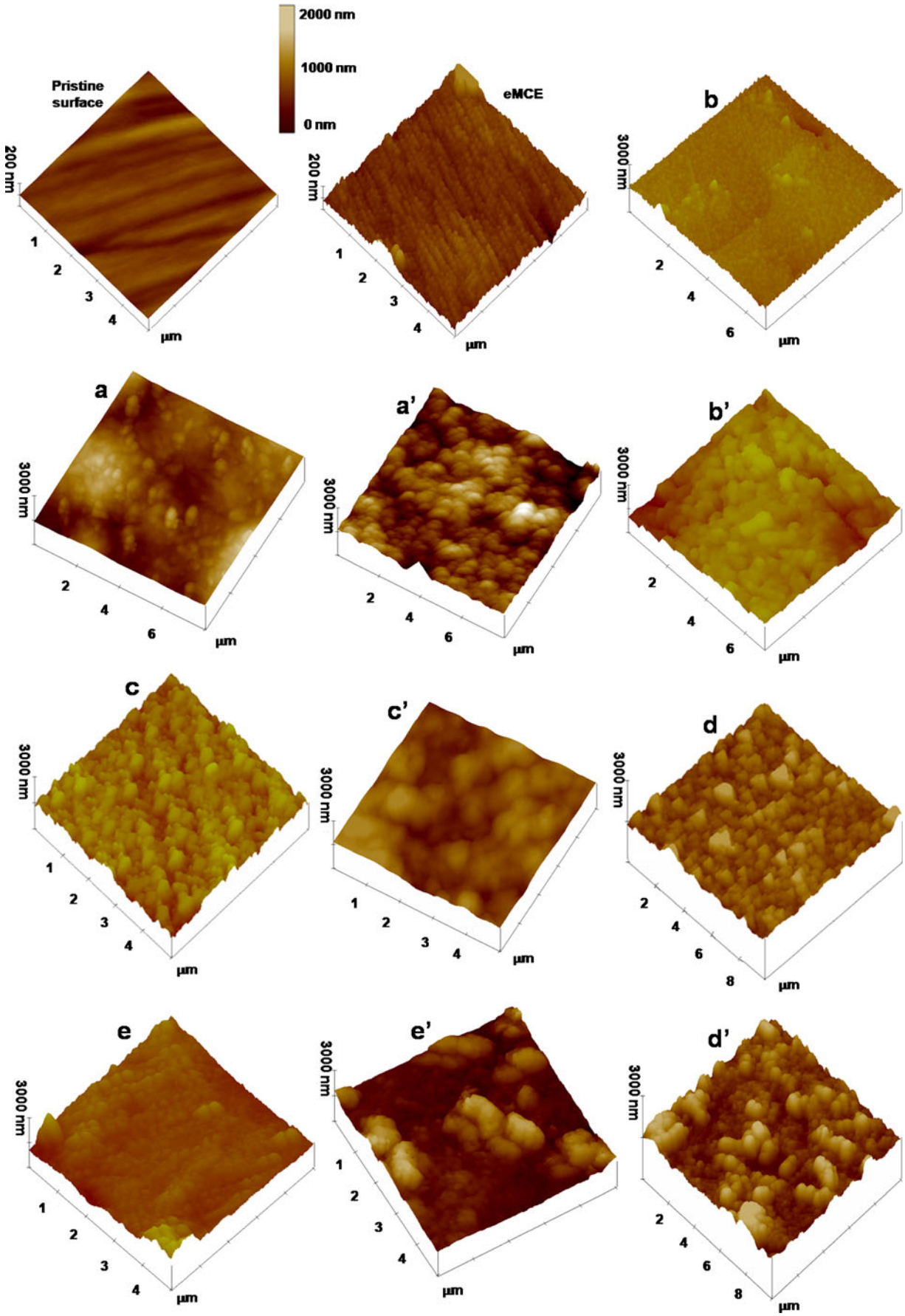
2000 nm
1000 nm
0 nm
Pristine surface
200 nm
1
2
3
4
µm
eMCE
200 nm
1
2
3
4
µm
b
3000 nm
2
4
6
µm
a
3000 nm
2
4
6
µm
a'
3000 nm
2
4
6
µm
b'
3000 nm
2
4
6
µm
c
3000 nm
1
2
3
4
µm
c'
3000 nm
1
2
3
4
µm
d
3000 nm
2
4
6
8
µm
e
3000 nm
1
2
3
4
µm
e'
3000 nm
1
2
3
4
µm
d'
3000 nm
2
4
6
8
µm

◀ **Fig. 2** AFM images of eMCE from the abiotic assays after 1 h (*a*), 12 h (*b*), 24 h (*c*), 48 h (*d*), and 120 h (*e*) and the time-corresponding eMCE from biotic assays (*a′* to *e′*). Images were acquired in air using tapping mode and a scan rate of 0.5–1 Hz. The height of elements is shown in the figure

units (A.U.). It has been demonstrated that CLSM is useful to quantify EPS and that CLSM is more sensitive than the chemical extraction of EPS in young and less compact biofilms.

Finally, SEM (Phillips XL 30 coupled to EDS 460 EDAX) analysis of eMCE was also carried out after biotic and abiotic assays but only at 24 h because biofilm formation reaches its better conformation after this biooxidation time. The biofilms were previously treated by application of a critical point procedure in order to stabilize and preserve their structural properties: (a) The eMCEs with biofilm were treated with glutaraldehyde at 3–4 % (*v*/*v*) over 48 h at 4 °C and washed with phosphate buffer solution at pH 7.2, (b) the biofilm was fixed for 2 h with osmium tetraoxide and rinsed three times with buffer solution, (c) the biofilm was dehydrated by continuous washing with a series of ethanol solutions at increasing concentrations (30–100 %). Afterward, samples were transferred into a chamber of a critical point dryer (Samdri-795), and the dehydrated samples were analyzed by SEM.

Quantification of proteins in EPS of biofilms

Quantification of proteins composing EPS after 1, 12, 24, 48, and 120 h of microorganism colonization was carried out using the well-known Bradford method (modified by Lara et al. (2012a)). For the extraction of extracellular proteins, different eluents (NaCl, NaOH, Na_2EDTA, and the medium ATCC-125) were assayed, and the stain Alcian Blue (specific for polysaccharides) was used to evaluate the extraction efficiency of each eluent and the cell integrity. The medium ATCC-125 showed the highest extraction efficiency. The biofilms of *A. thiooxidans* were scraped from each eMCE and placed on Eppendorf vials under iced conditions (4 °C). The vials were left inundated with 300 μL of ATCC-125 medium. Afterward, the vials were centrifuged during 15 min (5,000 rpm) under controlled temperature (4 °C), and the obtained pellets were resuspended using 300 μL of ATCC-125.

Bradford reaction was promoted by adding 3 mL of Bradford reagent into vials and mixing until homogeneous solutions were achieved; subsequently, the vials were placed in water bath for 15 min (30 °C). Protein quantification was carried out by comparing UV measurements (UV–visible spectrophotometer 50 Bio) with a reference curve using albumin as standard at concentrations between 1 and 30 mg/mL. All materials and solutions were previously sterilized by autoclaving and/or UV irradiation; analyses were performed in triplicate.

An electrophoresis analysis was performed to determine the weight of the extracted extracellular proteins after 120 h using polyacrylamide gel according to Laemmli (1970) and using an electrophoresis chamber (BIO-RAD mini protean, three cells 525 BR). Protein Ladder (Bench Marker) was used as molecular weight size marker. Proteins in the gel were fixed with acetic acid and simultaneously stained; for protein visualization, the anionic stain Coomassie Brilliant Blue (Sigma R-250) and a photodocumentator (BIO-RAD Universal Hood II) were used.

Results

Raman analysis showed the sulfur speciation on eMCEs' surfaces (Fig. 1; Table 1). In all cases, Raman peak at around 289 cm^{-1} indicates unmodified chalcopyrite (Fig. 1—f), while peaks at around 150 and 217 cm^{-1} indicate the formation of S^0 phases, and the broad Raman peak asymmetry at around 471 cm^{-1} (Fig. 1—g) indicates the formation of minor amounts of inactive S_n^{2-} (e.g., $Cu_{1-x}Fe_{1-y}S_2$; Table 1) together with S^0-like phases. The eMCE surfaces before the assays initially contained a mixture of active secondary S_n^{2-} and S^0 phases; S^0 phases are predominant and susceptible to biological oxidation (Lara et al. 2012b).

Raman spectra from the eMCE surface after 1 h of abiotic control showed the presence of S_n^{2-}, according with the Raman peak position and its course shape at around 471 cm^{-1} (Fig. 1—a; Table 1). However Raman spectra collected for the eMCE at the same time but in the biotic assay showed different and increased S_n^{2-} phases as indicated by the coarse peaks at 447–468 cm^{-1} (Fig. 1—a′; Table 1), which are also a clear sign of S_n^{2-} formation (Mycroft et al. 1990). These results indicated the surface transformation of the eMCE with total depletion of S^0, resulting in a wide range of S_n^{2-} phases on biooxidized eMCE (Fig. 1—a′).

After 12 h in the abiotic control, the Raman spectra of the eMCE show the formation of crystallized S^0 phases as indicated by the peaks at 150, 216, and 470 cm^{-1} (Fig. 1—b; Table 1). In contrast, in the presence of *A. thiooxidans*, a coarse peak at 468 cm^{-1} remains, indicating the persistence of S_n^{2-} on eMCE (Fig. 1—b′; Table 1).

After 24 h, the formation of S^0 phases was observed again on the eMCE of the abiotic control (149, 217, and 472 $cm^{-1;}$ Fig. 1—c; Table 1) as after 12 h and before leaching (Fig. 1—b, g, c, respectively). After 24 h of biotic assay, intense and sharp peaks were observed at 150, 219, and 452–473 cm^{-1}, which evidenced the formation of a more structured S_n^{2-} and S^0 during chalcopyrite biooxidation (Fig. 1—c′; Table 1), as well as a significant stage of diverse S_n^{2-} formation during the pathway of S^0 biooxidation.

Table 2 Evolution of roughness (R_a) and root mean square (R_q) values collected at different times on eECM areas in biotic and abiotic (control) assays. The R_q and R_a of eECM from biotic assays were obtained at the surrounding areas of the attached cells (n=50±standard deviation)

Time (h)	R_a (nm)		R_q (nm)	
	Biotic	Abiotic	Biotic	Abiotic
1	623.77±154.90	34.32±4.32	743.18±156.84	38.24±6.51
12	203.20±48.93	61.48±20.11	263.43±55.86	80.35±23.95
24	155.67±45.41	101.17±24.38	211.21±61.15	134.91±29.86
48	111.20±16.42	58.19±14.05	141.90±25.20	78.17±16.60
120	137.50±18.77	159.89±12.65	175.92±23.85	203.36±18.32

The abiotic control eMCEs' surfaces after 48 h (Fig. 1—d) and 120 h (Fig. 1—e) showed mainly S_n^{2-} and S^0 phases, respectively (Table 1), while in the biotic assays the corresponding Raman spectra indicate the biooxidation of S_n^{2-} to form copper-sulfide phases (e.g., CuS) (472–473 $cm^{-1;}$ Fig. 1—d′ and 1e′, respectively; Table 1). This comprises the most significant stage of eMCE modification due to *A. thiooxidans* activity and puts on evidence of new sceneries for chalcopyrite biooxidation at 120 h.

The eMCEs' surfaces used for the Raman study were then analyzed by AFM (Fig. 2). The eMCE from the biotic assays presented significantly higher values of roughness (R_a) than those from abiotic trials (Fig. 2; at a significance level of $p<0.05$ for $n=50$) in almost all the assayed times except at 120 h (Table 2). At the first hour of contact between *A. thiooxidans* and the eMCE, the R_a and R_q as well as Raman results suggested the biooxidation of the previously generated S_n^{2-} and S^0 by electrooxidation of MCE, resulting in the occurrence of two types of S_n^{2-} involving different structures (Fig. 1—f′), which confirmed the biological activity of *A. thiooxidans* since 1 h of contact time. Afterward, the R_a and R_q on the eMCEs' surfaces exposed to the microorganism progressively decreased concomitant with the total depletion of S^0 and S_n^{2-} (Fig. 1—a′).

Surprisingly, after 12 and 48 h, the R_a and R_q of the biotic assays were significantly higher than the R_a and R_q of their abiotic controls; meanwhile after 24 and 120 h, the R_a and R_q of both eMCEs' surfaces, biotic and abiotic, have the same order of magnitude (no significance differences) (Table 2). The lowest R_a and R_q of biotic trials occurred after 48 and 120 h; this was maybe because of the absence of S^0 on both eMCEs' surfaces and the formation of Cu secondary phases (Fig. 1—d, d′, e, and e′) within the matrix structure of chalcopyrite. The lowest R_a and R_q of biotic trials obtained after the AFM analysis (Fig. 2) are consistent with the cyclic (chemical) generation and (biological or chemical) oxidation of S^0 and S_n^{2-} as seen by the Raman analysis (Fig. 1); also, AFM images of eMCE suggested variable amounts of attached cells (Fig. 2—d′ and e′).

Although the AFM images (Fig. 2) suggest the presence of biofilms, the CLSM study confirmed a high cell density within the biofilm attached to the eMCE (Fig. 3). The

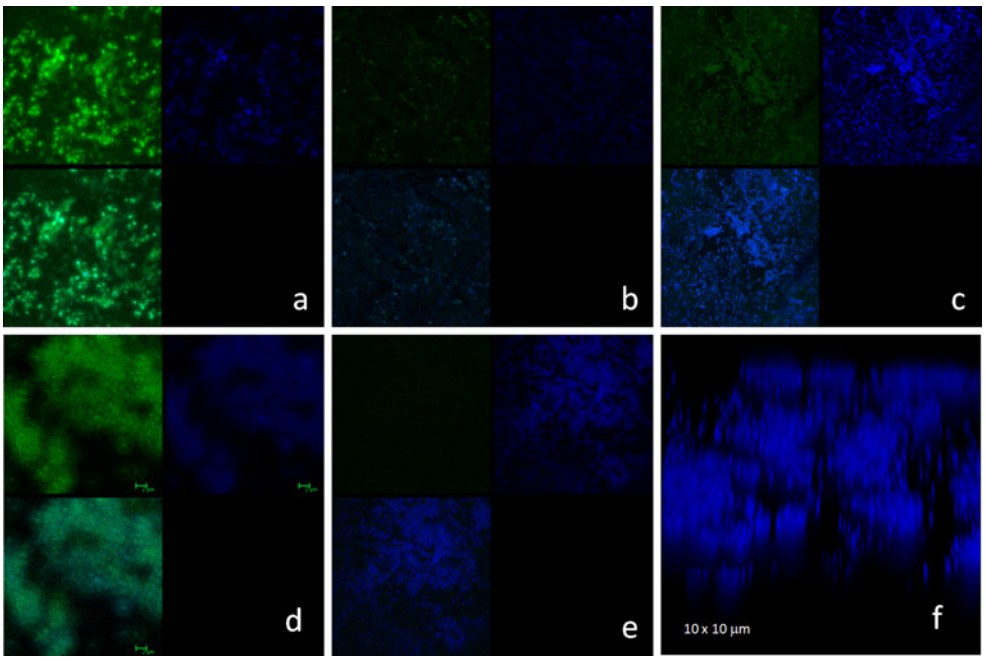

Fig. 3 CLSM images of *A. thiooxidans* biofilms (2D) formed after the biooxidation of eMCE's surfaces at different bioleaching times: 1 h (**a**), 12 h (**b**), 24 h (**c**), 48 h (**d**), and 120 h (**e**); CLSM image (3D) after 120 h (**f**). Epifluorescence of exopolysaccharides is shown in *green* and of lipids in *blue*; an overlap of both epifluorescence images is presented in the *lower left side* of the images (**a** to **e**)

formation of a thick and stratified biofilm initiated immediately after 1 h of *A. thiooxidans* exposure to eMCE, and a dense and multilayered biofilm was observed after 24 h (Fig. 3c, d).

Epifluorescence analysis of the EPS of biofilms indicates continuous and progressive secretion of hydrophilic exopolysaccharides and hydrophobic domains (as lipids) for the five stages associated with biofilm evolution (Fig. 3; Table 3), but with maximum epifluorescence emission at different colonization stages: at 1 h for hydrophilic exopolysaccharides and at 120 h for hydrophobic EPS (lipids). The obtained epifluorescence of extracellular polysaccharides and the epifluorescence of lipids were similar since 1 to 48 h; however, after 120 h, the epifluorescence of extracellular hydrophobic EPS was significantly higher than the epifluorescence of exopolysaccharides (161 and 13 A.U., respectively; Table 3; Fig. 3e).

Quantification of extracellular proteins completed the understanding of the biofilm compositions for the five stages during biofilm evolution (Table 4). A progressive increase and significant differences of extracellular proteins production ($p<0.05$ for $n=3$) were found at each time; the highest production and secretion of proteins was recorded at 120 h (43.47 mg). The electrophoresis analysis showed that the extracellular proteins secreted by biofilms of *A. thiooxidans* attached to the eMCE throughout 120 h are mainly of about 40 kDa (Fig. 4).

Finally, SEM observations and EDS analysis to the biofilm on eMCE after 24 h indicated the presence of biofilms and sulfur phases in the eMCE surfaces (Fig. 5), in agreement with Raman and AFM analysis.

Discussion

A. thiooxidans colonizes the surface of the eMCE which initially contained a mixture of active secondary S_n^{2-} and S^0 phases, with the S^0-like form being the predominant one. The microbiological biooxidation of these phases on eMCE improved the chemical process since the total consumption of S^0 in the abiotic assays initiated after 48 h, whereas biooxidation initiated since the first hour. The microorganism forms thick biofilms, with high density of cells and relatively high epifluorescence of hydrophilic polysaccharides and hydrophobic domains as lipids, since the first hour of exposure and throughout 120 h of assay time. After 120 h of colonization of the eMCE, the biofilm increases as well as the epifluorescence of EPS, and *A. thiooxidans* biooxidizes the S^0/S_n^{2-} on the eMCE surface, modifying the crystalline topography or texture, as indicated by Raman and AFM analyses (Figs. 1 and 2). *A. thiooxidans* colonizes eMCE actively, although in the absence of the IOMs *Acidithiobacillus ferrooxidans* or *Leptospirillum ferrooxidans*, and this is a clear evidence of the periodic biooxidation/formation of S^0/S_n^{2-}. The formation of these sulfur phases

Table 3 Epifluorescence values (A.U.) of extracellular polysaccharides and lipids of *A. thiooxidans* biofilms obtained using CLSM throughout the five stages of eMCE colonization performed ($n=30\pm$ standard deviation)

Time (h)	Polysaccharides	Lipids
1	88±11	88±10
12	32±1	32±4
24	35±2	39±7
48	149±42	109±34
120	13±2	161±25

Table 4 Quantification of proteins of the extracted EPS from *A. thiooxidans* biofilms attached on eMCE after the selected assay times

Time (h)	Proteins (mg/L)
1	0.25
12	1.99
24	1.69
48	2.28
120	3.47

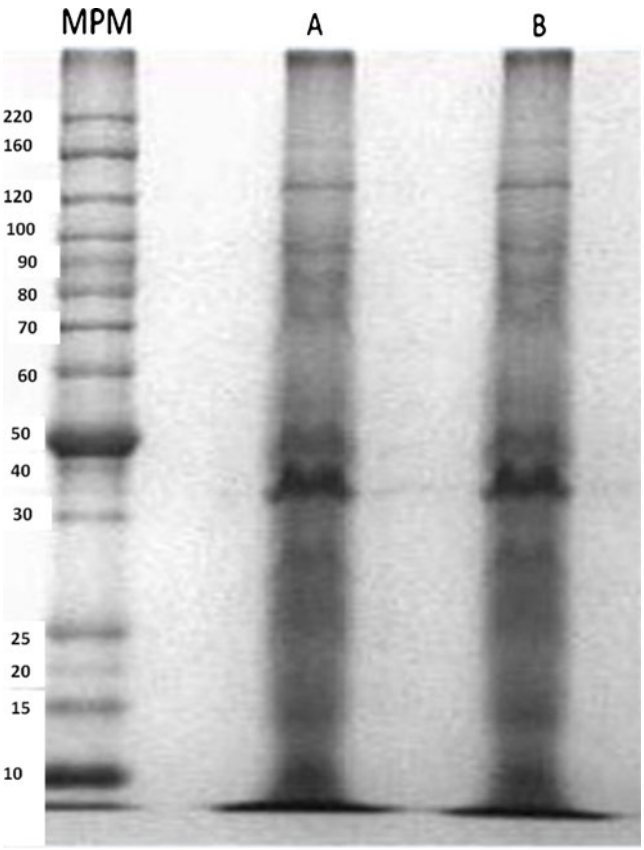

Fig. 4 Bidimensional SDS–polyacrylamide gels of the extracellular proteins extracted after 120 h of *A. thiooxidans* biofilm and eMCE interaction. *MPM* molecular weight marker

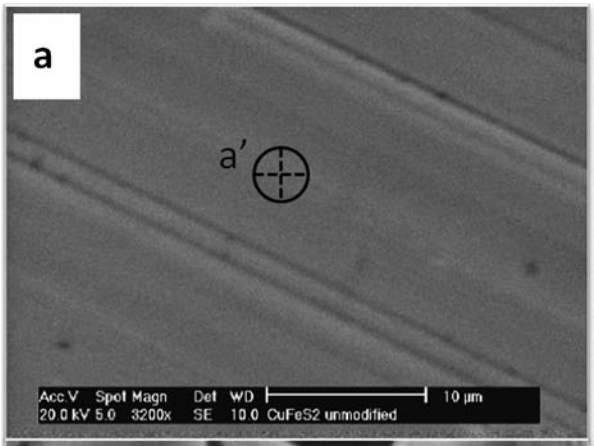

a′

Element	Wt %	At %
S K	30.16	44.6
FeK	31.85	27.05
CuK	37.99	28.35
Total	100	100

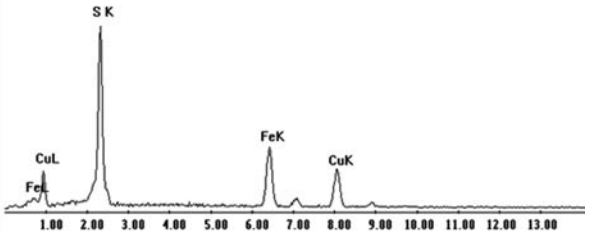

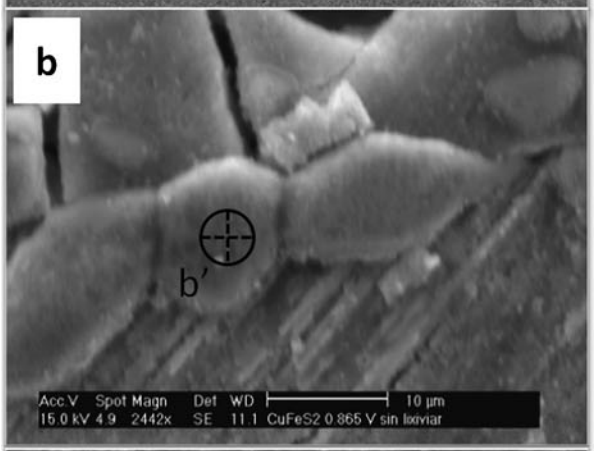

b′

Element	Wt %	At %
S K	100	100
Total	100	100

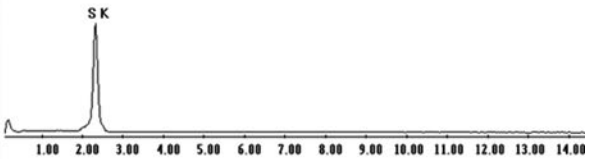

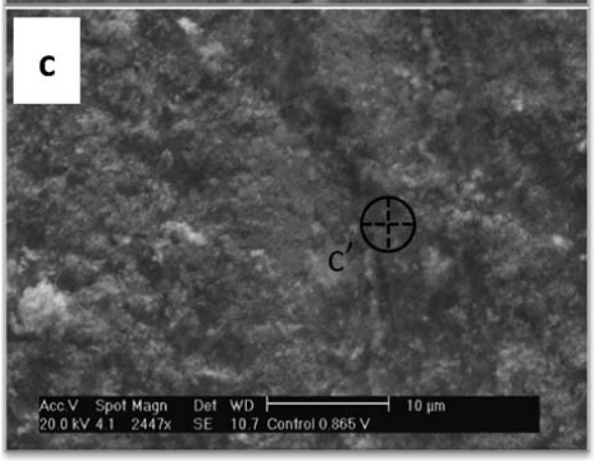

c′

Element	Wt %	At %
S K	100	100
Total	100	100

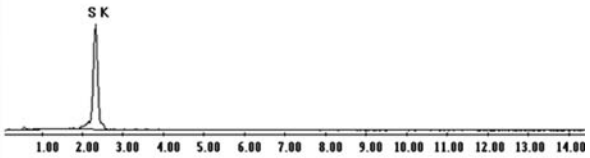

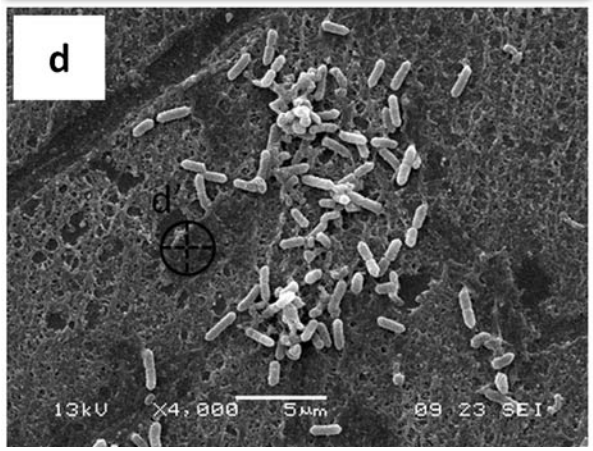

d′

Element	Wt %	At %
CuL	28.54	19.95
S K	39.38	54.54
FeK	32.08	25.51
Total	100	100

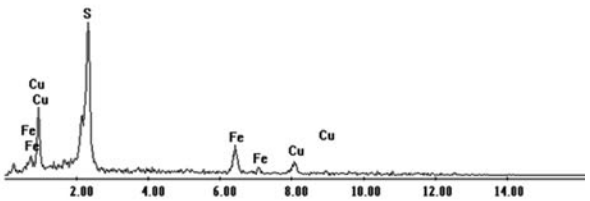

◀ **Fig. 5** SEM images and EDS spectra for different MCE surfaces: unmodified (*a*), before assays (*b*), after 24 h of incubation in abiotic control (*c*), and biotic trial (*d*). The marks indicate the region where the EDS analyses were done. The at.% at each region is also shown for comparison purposes

happens because chalcopyrite is an acid-soluble mineral subject to proton attacks, resulting in the production of ca. 90 % of S^0/S_n^{2-} (Schippers and Sand 1999). To compare assays with massive electrodes of the acid-insoluble pyrite (eMPEs), the biofilms of *A. thiooxidans* progressively decrease after 72 h, and only dispersed attached cells were observed; meanwhile, total biooxidation of S^0/S_n^{2-} occurred (González et al. 2012). Additionally, the concomitant formation of CuS phases on biooxidized eMCE after 48–120 h resulted in a favorable surface condition allowing biofilm stratification (e.g., Figs. 2 and 3c, d) due to the fact that CuS promotes the formation of S^0 clusters.

The AFM images of biotic trials (Fig. 2) confirm the spectra obtained by Raman and indicated that the R_a and R_q values are a consequence of periodical biooxidation/formation of S^0/S_n^{2-} due to biooxidation of S^0, a slower biooxidation of S_n^{2-} (even when some sulfur species are refractory), and covellite formation; it is important to note the absence of covellite in abiotic control. All these interfacial transformations on the eMCEs' surface occur; meanwhile, the epifluorescence of extracellular polysaccharides and hydrophobic domains (as lipids) increased. The highest EPS amount occurred after 48 h (polysaccharides) and 120 h (lipids), just when covellite was evident (Tables 1 and 3).

The transformation of the eMCEs' surface induces changes in the structure of *A. thiooxidans* biofilm since the cells respond to the spatial and temporal distribution of the sulfur phases, evolving to a multilayered biofilm after 120 h (Fig. 3e, f). Similar results were observed using eMPE (González et al. 2012); however, in this work with eMCE, we did not detect a transition from dispersed colonies of cells to a well-stratified biofilm, but from mono- to multilayered biofilm. According to the "Non-homogenous Biofilm Modeling" of Olivera-Nappa et al. (2010), microorganisms of biofilms set in a sulfur substrate grown at higher rates create "flat" (mono- or bilayered) biofilms instead of fungi- or dome-shaped biofilms. In general, *A. thiooxidans* forms flat biofilms on eMPE (González et al. 2012) and eMCE (this study) when a mixture of active secondary S_n^{2-} and S^0 phases are present on the surface of chalcopyrite, as demonstrated by the Raman analyses. Probably, a flat biofilm represents the typical structure of SOM biofilms "in response to the intrinsic chemical reactivity of minerals that produce sulfur under oxidative leaching conditions, like chalcopyrite" (Olivera-Nappa et al. 2010).

The transformation of eMCE also induces changes in EPS compositions, e.g., covellite is colonized and biooxidized by SOM if the cells become hydrophobic (Pogliani and Donati 1999; Falco et al. 2003). In EPS and after 120 h, the hydrophobic domains achieved their highest amount, as well as proteins of about 40 kDa (Table 3; Fig. 4), confirming EPS modifications associated with surface chemical evolution. Bobadilla et al. (2011) reported that the major protein secreted by *A. thiooxidans* cultured with elemental sulfur is the 42.2-kDa lipoprotein Licanantase. Licanantase is an Omp40-like protein involved in the adherence to hydrophobic surfaces as sulfur particles and in electron transport. Adhesion and electron transport "are key aspects in bacterial colonization and biooxidation of insoluble substrates" (Bobadilla et al. 2011).

If the biooxidation of S^0/S_n^{2-} and covellite requires direct contact between cells and sulfur (Takakuwa et al. 1977; Fowler and Crundwell 1999; Liu et al. 2003; Rohwerder et al. 2003; Lara et al. 2010), the cells must first overcome the hydrophobic barrier between the colonized sulfur particles (Arredondo et al. 1994; Gehrke et al. 1998; Pogliani and Donati 1999; Zhang et al. 2009). Hydrophobic secretion brings down the interfacial tension between cells and the surface with sulfur (Devasia et al. 1993; Natarajan and Das 2003; Devasia and Natarajan 2010). The former may explain why the epifluorescence of extracellular polysaccharides and lipids was similar until 48 h (Table 3). Zhang et al. (2009) demonstrated that the surface of *A. ferrooxidans* cultured with insoluble S^0 contained more abundant and polar functional groups (−CONH–, –COOH, and –NH–) than those cultured with soluble thiosulfate as their Fourier transform infrared spectroscopy analysis showed. Additionally, Devasia and Natarajan (2010) suggested that the polysaccharide moieties in EPS are favored when the cells are utilizing soluble substrates, but the exposure of hydrophobic domains occurred when cells were grown on minerals.

The corollary of the former is well expressed by Zhang et al. (2009): "So it is certainly reasonable to infer that the lipopolysaccharides and proteins of the EPS and outer membrane may be responsible for overcoming the hydrophobic barrier during sulfur surface modification and oxidation". Our results support the suggestion of Zhang and collaborators and indicate a relationship between structure and function of the biofilm with the distribution and transformation of sulfur phases.

The high content of hydrophobic EPS at 120 h also seems related with the increase of cell number and consequently with the thickness of biofilms. According to Zeng et al. (2010), the large amount of EPS formed by IOM and SOM on the chalcopyrite surface after 16 days mediated the precipitation of jarosite and $PbSO_4$ on the mineral surface, which enhances the formation of passivation layers and obstructs copper extraction. Sasaki et al. (2009) found jarosite, covellite, and S^0 in the passive layer when the media contain Fe^{3+} produced by the IOM *A. ferrooxidans* after 18 days; Lei et al. (2009) observed biofilms of *A. ferrooxidans* on chalcopyrite that was covered by jarosite

and S^0 after 15 days, a cover that seems to cause the death of the cells. Conversely, in our short-term experiment, no passive layers were detected, emphasizing the importance of SOM activity but suggesting that bioleaching may progress at shorter residence times. Lara et al. (2012b) had already suggested that cells of *A. thiooxidans* may grow as a flat and stratified biofilm even if the cells are partially covered by covellite and S^0 during the biooxidation of chalcopyrite.

Acknowledgments Financial support for this work comes from the Mexican Council of Science and Technology (CONACyT) (Project No. 05–49321). This work is also part of an outgoing collaboration between UJED (CA-UJED-105), UASLP (CA-UASLP-178), and UAM-I (UAM-I-CA-34). We thank Dr. Amauri Pozos and Keila N. Alvarado for the CLSM analysis (Basics Sciences Laboratory, UASLP), Dr. Jaime Ruiz-García and D. Valdez-Pérez for the AFM analysis (Colloids and Interfaces Laboratory, Institute of Physics, UASLP), Erasmo Mata-Martínez (Institute of Geology, UASLP) for the preparation of chalcopyrite sections, and Francisco Galindo-Murillo (Institute of Metallurgy, UASLP) for MCE preparation.

References

Arredondo R, García A, Jeréz CA (1994) Partial removal of lipopolysaccharide from *Thiobacillus ferrooxidans* affects its adhesion to solids. Appl Environ Microbiol 60:2846–2851

Bobadilla RA, Levican G, Parada P (2011) *Acidithiobacillus thiooxidans* secretome containing a newly described lipoprotein Licanantase enhances chalcopyrite bioleaching rate. Appl Microbiol Biotechnol 89:771–780

Devasia P, Natarajan KA (2010) Adhesion of *Acidithiobacillus ferrooxidans* to mineral surfaces. Int J Miner Proces 94:135–139. doi:10.1016/j.minpro.2010.02.003

Devasia P, Natarajan KA, Sathyanarayana DN, Rao RG (1993) Surface chemistry of *Thiobacillus ferrooxidans* relevant to adhesion on mineral surface. Appl Environ Microbiol 59(12):4051–4055. doi:4051-4055

El Jaroudi O, Picquenard E, Demortier A, Lelieur JP, Corset J (1999) Polysulfide anions. 1. Structure and vibrational spectra of the S_2^{2-} and S_3^{2-} anions. Influence of the cations on bond length and angle. Inorg Chem 38:2394–2401. doi:10.1021/ic9811143

El Jaroudi O, Picquenard E, Demotier A, Lelieur JP, Corset J (2000) Polysulfide anions II: structure and vibrational spectra of the S_4^{2-} and S_5^{2-} anions. Influence of the cations on bond length, valence and torsion angle. Inorg Chem 39:2593–2603. doi:10.1021/ic991419x

Falco L, Pogliani C, Curutchet GE, Donati E (2003) A comparison of bioleaching of covellite using pure cultures of *Acidithiobacillus ferrooxidans* and *Acidithiobacillus thiooxidans* or a mixed culture of *Leptospirillum ferrooxidans* and *Acidithiobacillus thiooxidans*. Hydrometallurgy 71:31–36. doi:10.1016/S0304-386X(03)00170-1

Fowler TA, Crundwell FK (1999) Leaching of zinc sulfide by *Thiobacillus ferrooxidans*: bacterial oxidation of the sulfur product layer increases the rate of zinc sulfide dissolution at high concentration of ferrous ions. Appl Environ Microbiol 65(12):5285–5292

Gehrke T, Telegdi J, Thierry D, Sand W (1998) Importance of extracellular polymeric substances from *Thiobacillus ferrooxidans* for bioleaching. Appl Environ Microbiol 64:2743–2747

González DM, Lara RH, Alvarado KN, Valdez-Pérez D, Navarro-Contreras HR, García-Meza JV (2012) Evolution of biofilms during the colonization process of pyrite by *Acidithiobacillus thiooxidans*. Appl Microbiol Biotechnol. doi:10.1007/s00253-011-3465-2

Laemmli UK (1970) Cleavage of structural proteins during the assembly of the head of bacteriophage T4. Nature 227:680–685

Lara RH, Valdez-Pérez D, Rodríguez AG, Navarro-Contreras HR, Cruz G-MJV (2010) Interfacial insights of pyrite colonized by *Acidithiobacillus thiooxidans* cells under acidic conditions. Hydrometallurgy 103:35–44. doi:10.1016/j.hydromet.2010.02.014

Lara RH, García-Meza JV, Cruz R, Valdez-Pérez D, González I (2012a) Influence of the sulfur species reactivity on biofilm conformation during pyrite colonization by *Acidithiobacillus thiooxidans*. Appl Microbiol Biotechnol 95:799–809. doi:10.1007/s00253-011-3715-3

Lara RH, García-Meza JV, González I, Cruz R (2012b) Influence of the surface speciation on biofilm attachment to chalcopyrite by *Acidithiobacillus thiooxidans*. Appl Microbiol Biotechnol. doi:10.1007/s00253-012-4099-8

Lee MS, Nicol MJ, Basson P (2008) Cathodic processes in the leaching and electrochemistry of covellite in mixed sulfate–chloride media. J Appl Electrochem 38:363–369. doi:10.1007/s10800-007-9447-5

Lei J, Huaiyang Z, Xiaotong P, Zhonghao D (2009) The use of microscopy techniques to analyze microbial biofilms of the bio-oxidized chalcopyrite surface. Mineral Eng 22:37–42

Liu HL, Chen BY, Lan YW, Cheng YC (2003) SEM and AFM images of pyrite surfaces after bioleaching by the indigenous *Thiobacillus thiooxidans*. Appl Microbiol Biotechnol 62:414–420. doi:10.1007/s00253-003-1280-0

Mycroft JR, Bancroft GM, McIntyre NS, Lorimer JW, Hill IR (1990) Detection of sulphur and polysulphides on electrochemically oxidized pyrite surfaces by X-ray photoelectron spectroscopy and Raman spectroscopy. J Electroanal Chem 292:139–152. doi:10.1016/0022-0728(90)87332-E

Natarajan KA, Das A (2003) Surface chemical studies on *Acidithiobacillus* group of bacteria with reference to mineral flocculation. Int J Miner Process 72:189–198. doi:10.1016/S0301-7516(03)00098-X

Olivera-Nappa A, Picioreanu C, Asenjo JA (2010) Non-homogeneous biofilm modeling applied to bioleaching processes. Biotechnol Bioeng 106(4):660–676. doi:10.1002/bit.22731

Parker GK, Woods R, Hope GA (2008) Raman investigation of chalcopyrite oxidation. Coll Surf A 318:160–168. doi:10.1016/j.colsurfa.2007.12.030

Pogliani C, Donati E (1999) The role of exopolymers in bioleaching of a non-ferrous metal sulphide. J Ind Microbiol Biotechnol 22 (2):88–92

Rohwerder T, Gehrke T, Kinzler K, Sand W (2003) Bioleaching review part A: progress in bioleaching: fundamentals and mechanisms of bacterial metal sulfide oxidation. Appl Microbiol Biotechnol 63:239–248. doi:10.1007/s00253-003-1448-7

Sasaki K, Tsunekawa M, Ohtsuka T, Konno H (1998) The role of sulfur-oxidizing bacteria *Thiobacillus thiooxidans* in pyrite weathering. Colloid Surface A 133:269–278. doi:10.1016/S0927-7757(97)00200-8

Sasaki K, Nakamuta Y, Hirajima T, Tuovinen OH (2009) Raman characterization of secondary minerals formed during chalcopyrite leaching with *Acidithiobacillus ferrooxidans*. Hydrometallurgy 95:153–158. doi:10.1016/j.hydromet.2008.05.009

Schippers A, Sand W (1999) Bacterial leaching of metal sulfides proceeds by two indirect mechanisms via thiosulfate or via polysulfides and sulfur. Appl Environ Microbiol 65:319–321

Takakuwa S, Nishikawa T, Hosoda K, Tominaga N, Iwasaki H (1977) Promoting effect of molybdate on the growth of a sulfur oxidizing bacterium, *Thiobacillus thiooxidans*. J Gen Appl Microbiol 23:163–173

Toniazzo V, Mustin C, Portal JM, Humbert B, Benoit R, Erre R (1999) Elemental sulfur at the pyrite surfaces: speciation and quantification. Appl Surf Sci 143:229–237. doi:10.1016/S0169-4332(98)00918-0

Turcotte RE, Benner AM, Riley J, Li M, Wadsworth E, Bodily DM (1993) Surface analysis of electrochemically oxidized metal sulfides using Raman spectroscopy. J Electroanal Chem 347:195–205. doi:10.1016/0022-0728(93)80088-Y

Xia JL, Yang Y, He H, Liang CL, Zhao XJ, Zheng L, Ma CY, Zhao YD, Nie ZY, Qiu GZ (2010) Investigation of the sulfur speciation during chalcopyrite leaching by moderate thermophile *Sulfobacillus thermosulfidooxidans*. Int J Mineral Process 94:52–57. doi:10.1016/j.minpro.2009.11.005

Zeng W, Qiu G, Zhou H, Liu X, Chen M, Chao W, Zhang C, Peng J (2010) Characterization of extracellular polymeric substances extracted during the bioleaching of chalcopyrite concentrate. Hydrometallurgy 100:177–180. doi:10.1016/j.hydromet.2009.11.002

Zhang C-G, Xia J-L, Ding J-N, Ouyang X-D, Nie Z-Y, Qiu G-Z (2009) Cellular acclimation of *Acidithiobacillus ferrooxidans* to sulfur biooxidation. Mineral Metall Proc 26:30–34